

NEW INVESTIGATIONS APPLIED ON CADMIUM SULFIDE THIN FILMS FOR PHOTOVOLTAIC APPLICATIONS

O. TOMA, S. IFTIMIE, C. BESLEAGA, T. L. MITRAN, V. GHENESCU,
O. PORUMB, A. TODERAS, M. RADU, L. ION, S. ANTOHE*
*University of Bucharest, Faculty of Physics, 405 Atomistilor Street, PO Box
MG-11, 077125, Magurele-Ilfov, Romania*

In this paper we present some new investigations made on nanocrystalline cadmium sulfide thin films used as photoactive components in CdS/CdTe photovoltaic cells. The cadmium sulfide (CdS) thin films were deposited by method of thermal vacuum evaporation, from a single source, on ITO covered optical glass substrates of different thicknesses and electrical resistances. In order to improve the structural and chemical properties of the prepared films, post-deposition thermal treatments combined with chemical treatments based on CdCl₂ vapors were performed on all samples. The transmission as well as the absorption spectra were recorded using a UV-VIS double beam spectrophotometer. From the absorption spectra, the optical band-gaps of the films were calculated. The structural characterization of the cadmium sulfide thin films was made by GIXRD (Grazing Incidence X – Ray Diffraction) for samples of different thicknesses. The morphological investigations were carried out by cross section SEM (Scanning Electron Microscopy) for a more detailed evaluation of the CdS thin films. Finally the investigations were completed with electric measurements of the obtained photovoltaic devices.

(Received December 12, 2011; accepted December 20, 2011)

Keywords: Thin films photovoltaics, Optical absorption spectrophotometry, GIXRD, Cross section SEM, Electric measurements.

1. Introduction

In recent years a significant interest is associated with the A_{II}–B_{VI} semiconductor compounds, due to their novel properties and large area of applications. Various nanostructures made out from A_{II}–B_{VI} semiconductor compounds have been made, such as nanowires, nanorods, nanotubes, nanobelts, etc., with wide range of applications, especially in electronics and optoelectronics devices, where the techniques for the manipulation of the electrical and optical properties, doping and free carriers transport properties are intensely discussed [1-16].

Among these semiconductor compounds, CdS is one of the widely studied materials [1–10]. This material has many applications and from these applications we are interested in photovoltaic applications, in particular in manufacturing high efficiencies heterojunction CdS/CdTe solar cells. A substantial number of experimental efforts have been made so far in order to improve the efficiencies of these experimental cells [17–22]. However the efficiencies for the solar energy conversion are still relatively low, despite the theoretical calculations that suggests a maximum achievable efficiency of 30 % for CdTe solar cells.

The increased interest for this kind of solar cells is also due to their use in space technologies, where a considerable amount of work has been done in characterizing various properties of CdS/CdTe photovoltaic cells after their irradiation with different ionizing radiations [23-25].

*Corresponding author : santohe@solid.fizica.unibuc.ro

Experimental details about the deposition conditions, post-deposition thermal and chemical treatments and characterizations are given in the next section. The experimental results and their discussions are presented in section 3 and in the last section the main conclusions of this work are summarized.

2. Experimental details

We prepared polycrystalline CdS thin films by thermal vacuum evaporation (TVE) deposition method. All the CdS thin films were deposited on ITO and IZO covered optical glasses as substrates. The CdS powder (Aldrich) sublimates at a deposition pressure of 3.2×10^{-4} mbar inside the deposition chamber, from a single quartz crucible heated at 740 °C. This crucible was covered with a quartz-wool plug in order to prevent the CdS powder sputtering during the sublimation process. The substrate temperature was maintained constant at 250 °C [26].

After the CdS thin films deposition, the samples were subjected to a thermal treatment consisting in heating at 350 °C in vacuum for 18 minutes. The aim of this post-deposition thermal treatment is to improve the structural and chemical properties of these thin films.

In order to investigate the electrical properties of the entire photovoltaic device composed by CdS and CdTe thin films, a CdTe layer (thickness around 3.5 μm) were deposited, also by thermal vacuum evaporation in the same chamber, by sublimation of CdTe powder (Aldrich), when the quartz container was heated at 600° C [27]. The substrate was maintained at 250° C. The next technological step was again the thermal treatment, the whole structure being heated at 350° C for 18 minutes.

After this thermal treatment, the ITO (or IZO) / CdS / CdTe / samples were subjected to a series of chemical treatments based on CdCl₂ vapors. These chemical post-deposition treatments are very important for obtaining a good photovoltaic activity [28] as well as for improving the qualities of the components layers. Two kind of chemical treatments have been employed: a dry CdCl₂ treatment, respectively, a wet CdCl₂ treatment.

During the dry chemical treatment, the CdCl₂ powder (Aldrich) sublimated at a pressure of 10^{-5} Torr inside the deposition chamber from the quartz crucible heated at 250° C, temperature of the samples (used now as substrates for CdCl₂ vapors) being maintained constant at 100° C. As result of this evaporation a thin CdCl₂ layer (approx. 80 nm thickness) was obtained. After the deposition of cadmium chloride layer the entire structure was heated at 200° C for 20 minutes. The wet chemical treatment was made by immersing the samples in CdCl₂ solution (concentration is 2.08 g of CdCl₂ in 100 ml of methanol CH₃OH) for about 7 seconds. After this immersion the samples were heated in vacuum at 375° C for 30 minutes.

To complete the solar cell structure, a 50 nm copper layer and a 100 nm gold layer were deposited on top of the chemically treated CdTe layers, as back contacts. After the deposition of the copper layer an annealing treatment in vacuum at 150° C for 30 minutes was applied. Finally, after this procedure the gold layer was deposited (we used a silver paste to secure the electrical contacts to the electrodes). The active area of each solar cell was 0.4 cm².

The transmission as well as the absorption spectra were recorded using a double-beam spectrophotometer Perkin Elmer Lambda 35. The investigated spectral range was between 190 nm to 1.1 μm . For each sample the optical band gap values were measured directly from the absorption spectra. The structural properties for the CdS thin films were investigated using Grazing Incidence X-Ray Diffraction (GIXRD), using a Bruker D 8 Discover diffractometer.

The surface morphology for the CdS thin films were analyzed by Cross Section Scanning Electron Microscopy (Cross-Section SEM), using a Tescan Vega XMU-II microscope with secondary electrons as signal (the acceleration voltage was between 200 V up to 30 kV, the resulting magnification being from 3 x up to 500.000 x). The SEM had also an adjustable scanning speed between 160 ns / pixel to 10 ms / pixel.

Finally, the electric characterizations regarding the dark current-voltage (I-V) measurements were done at room temperature using a 2400 Keithley Source Meter. The range of

the sweeping voltage across the samples is set using lab view software which is connected with the source meter.

3. Results and discussion

First thing to do was to investigate the crystallographic structure using the X-ray diffraction technique. In Figure 1 are the XRD spectra for CdS thin films of three different thicknesses: 125 nm, 185 nm and 245 nm, respectively.

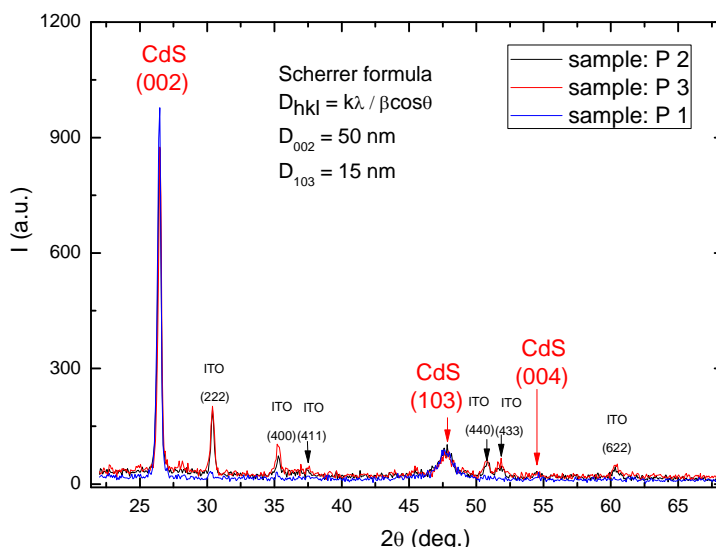


Fig. 1 – GIXRD spectra for CdS / ITO / optical glass: P1 = 125 nm, P2 = 185 nm, P3 = 245 nm

The identification of crystalline phases for the deposited CdS thin films, was made by grazing incidence X – ray diffraction (GIXRD), using a Bruker D 8 Discover diffractometer, in parallel beam setting, with monochromatised $\text{CuK}_{\alpha 1}$ radiation ($\lambda = 1.5406 \text{ \AA}$). We decided to work at grazing incidence (the incidence angle was set at 1.5°) in order to reduce the intensity of the radiation reflected (by diffraction) by the substrate. The scattered intensity was scanned in the 2θ range between $22 - 69^\circ$, with a step size of 0.08° at a rate of 1 second per step.

As we can see from the Figure 1, structural GIXRD analyses for all CdS/ITO/optical glass samples indicated that their structure consist of a hexagonal ZnO type crystalline phase (würtzite phase), preferentially oriented in the (002) direction. This direction corresponds to the c – axis, which is, in this case, the direction with the highest growth rate for the CdS thin films. The (103) line can be also observed for all samples.

Using Scherrer formula:

$$D_{hkl} = \frac{k\lambda}{\beta \cos \theta} \quad (1)$$

where the shape factor $k = 0.9$, λ is the X – ray wavelength, β the line broadening at half the intensity maximum (in radians) and θ the Bragg angle, we can easily calculate the size of crystallites. Thus the crystallite's size for the (002) direction was of almost 50 nm, as for the corresponding (103) reflection a size of about 15 nm was calculated.

For the surface morphology investigations we have used the Cross-Section SEM technique, using a Tescan Vega XMU-II SEM microscope. In order to perform this kind of analyses, we had to prepare more samples, different than the samples investigated by GIXRD. Those samples were: Sample 1 (S1) with the structure IZO coated optical glass / CdS/CdTe (dry

CdCl_2)/Cu/Au, Sample 2 (S2) with the structure ITO ($15 - 25 \Omega / \text{cm}^2$) coated optical glass/CdS/CdTe(dry CdCl_2)/Cu/Au and Sample 3 (S3) with the following material structure ITO ($8-12 \Omega / \text{cm}^2$)/CdS/CdTe (wet CdCl_2)/Cu/Au.

The corresponding Cross-Section SEM images for each sample are presented in the Figure 2. There are two rows, each row containing three SEM images (corresponding to each sample): the upper row contains SEM images recorded with a higher scanning speed, while the row below contains SEM images recorded with a smaller scanning speed. For images in the lower row the corresponding thicknesses for each layer are figured.

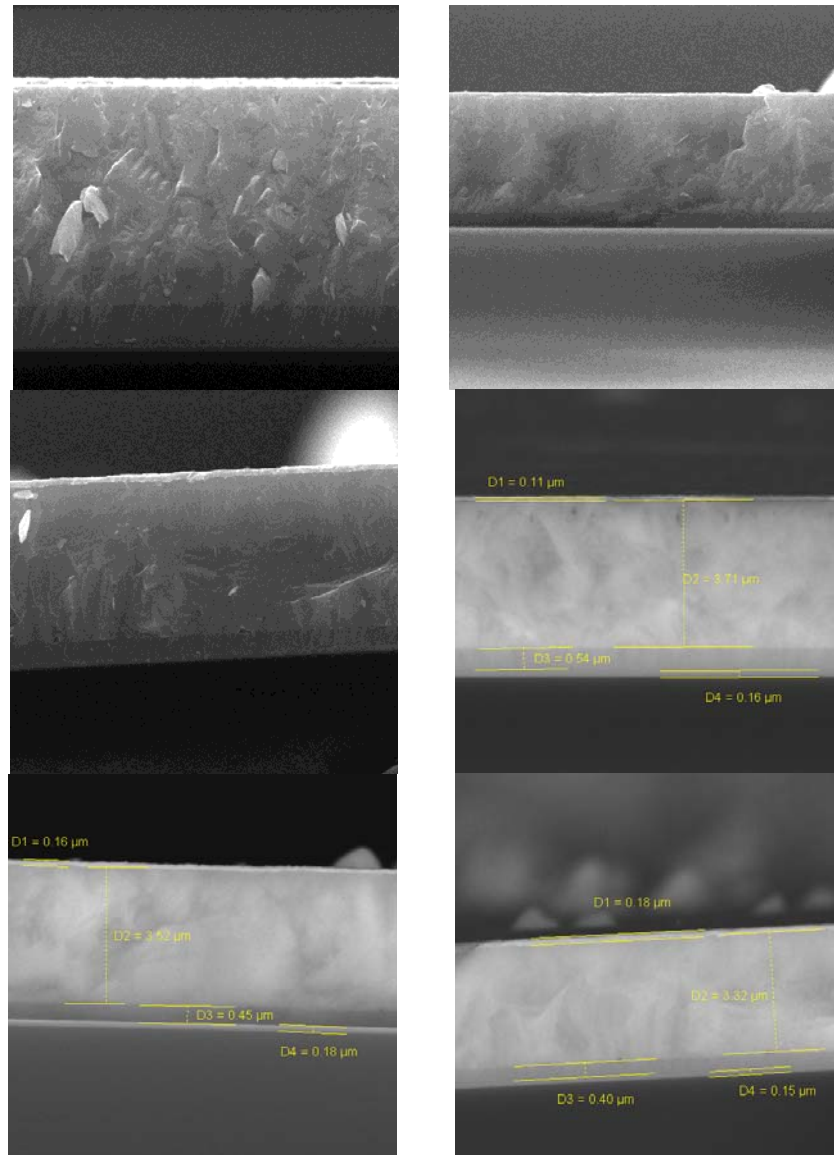


*Fig. 2 –Cross-Section SEM images for three samples:
S 1 – left images, S 2 – central images, S 3 – right images*

As we can see the thicknesses for CdS layers are between 400 nm (sample S 3) to 540 nm (sample S 1), as for the CdTe the corresponding thicknesses are situated between 3.32 μm (sample S 3) up to 3.71 μm (sample S 1).

We also can see from SEM images contained in the first row that the chemical treatment based on the use of CdCl_2 vapors on CdTe thin films, does not produce any significant modification on the grain sizes, in this sense thermal treatments seems to be more important.

However, the chemical treatments based on the interaction between CdTe thin layers and CdCl₂ reactive vapors, tends to lead at more smooth surfaces (for comparison, the left SEM image from the upper row correspond to S1 sample that has been chemically treated with dry CdCl₂, as the right SEM image from the upper row correspond to S3 sample, which has also chemically treated, but using this time wet CdCl₂ vapors). We expect that using multiple chemical treatments of the deposited CdS/CdTe photovoltaic structures, more rounded grain facets could be obtained.

The optical properties of the CdS thin films were investigated using a double-beam spectrophotometer Perkin Elmer Lambda 35. We recorded both transmission and absorption spectra for the next samples: samples P1, P2 and P3 are the same samples investigated by GIXRD, with the material structure ITO coated optical glass/CdS and three different thicknesses (125nm, 185 nm and 245 nm). Sample P4 has the structure IZO coated optical glass/CdS with the thickness 185 nm. All spectra were recorded at room temperature.

None of these material structures based on thin CdS films, were not subjected to any kind of chemical treatments using CdCl₂ vapors. We wanted first to investigate their intrinsic optical properties (transmission and absorption properties) as window materials and then, after the deposition of CdTe p-type films, we start the chemical treatments procedures.

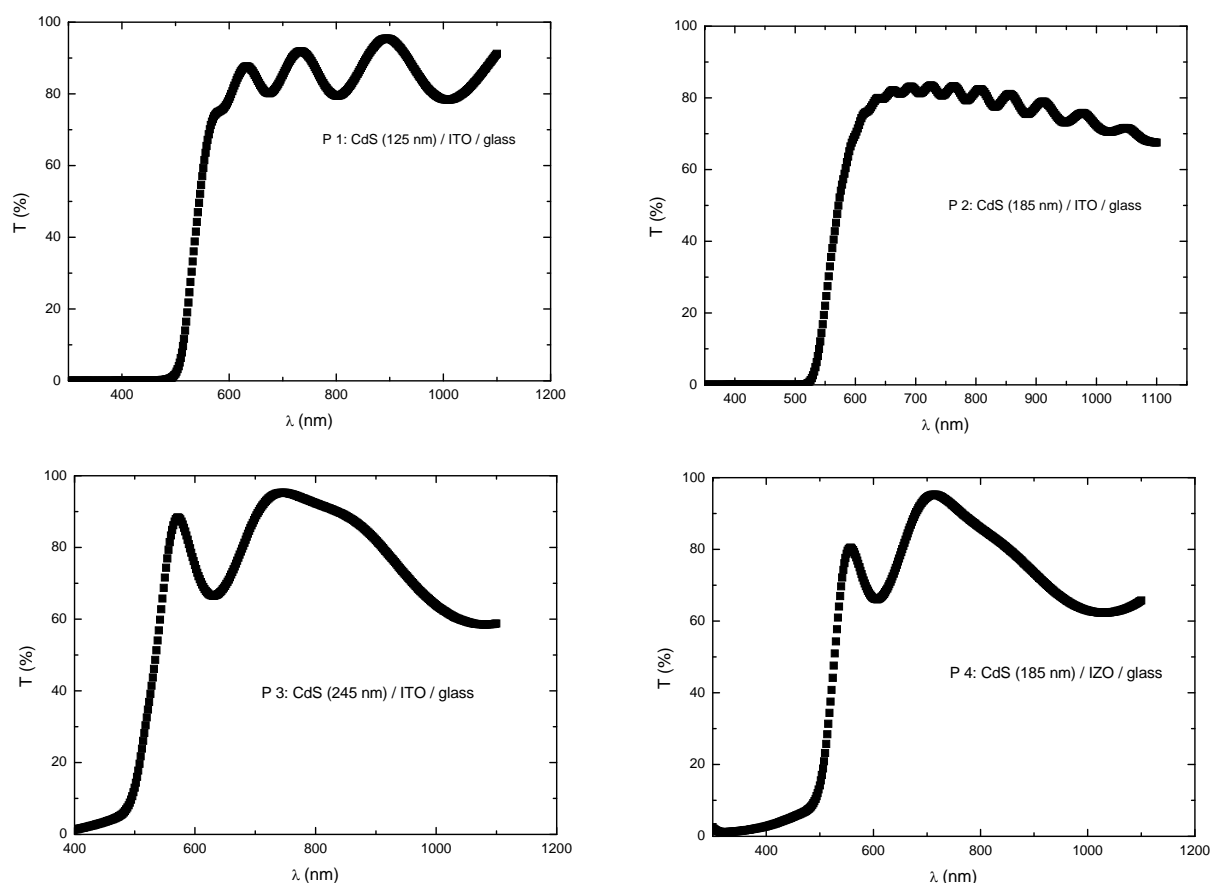


Fig. 3 – The transmission spectra

As we can see from the Figure 3 the optical transmittance for polycrystalline CdS thin films is higher than 60 % for all investigated samples.

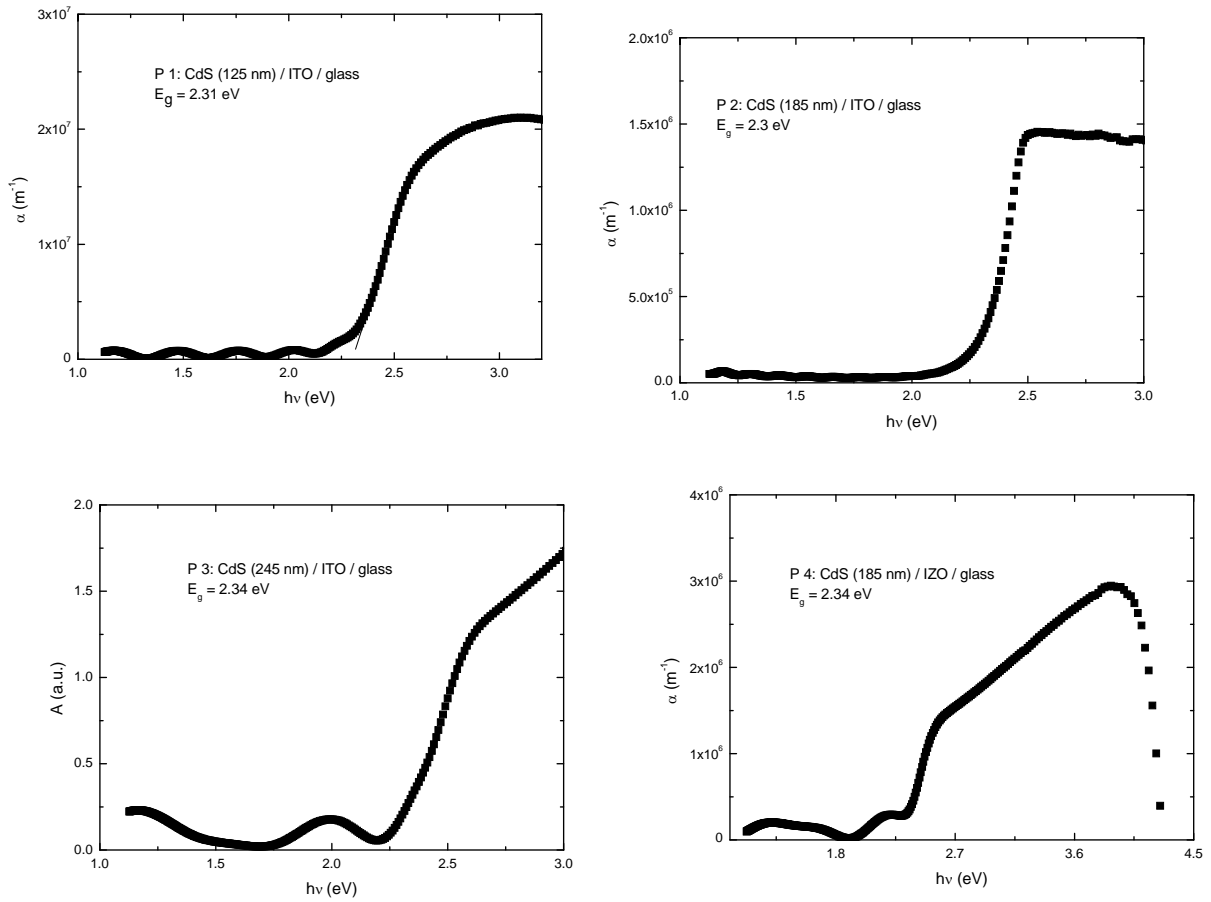


Fig. 4 – The absorption spectra of CdS thin films

The Figure 4 contains the absorption spectra of the four employed samples of CdS thin films, with the calculated values for the optical band gaps. Taking into account that CdS is a classic A_{II}-B_{VI} semiconductor compound with direct bands (direct transitions), the optical band gaps were relatively easy computed from the fundamental absorption region. We obtained values for the optical band gap between 2.3 eV and 2.34 eV, which are in good concordance with other reported results.

The final part of this paper is devoted to electric measurements of the obtained photovoltaic cells. Two samples were investigated as follows: P1 sample has the structure ITO (15–25 Ω/cm²) coated optical glass/CdS/CdTe (dry CdCl₂)/Cu/Au, while P2 sample has the material structure IZO/CdS/CdTe (wet CdCl₂)/Cu/Au.

The data were recorded using a 2400 Keithley Source Meter. The current-voltage characteristics of our solar cells treated in CdCl₂ have been measured in dark light, at room temperature, in both forward and reverse bias conditions, as they are shown in Figure 5. As expected, the forward bias conditions lead to an increase of the current density with the positive voltage between the gold electrode with respect to the ITO front contact electrode.

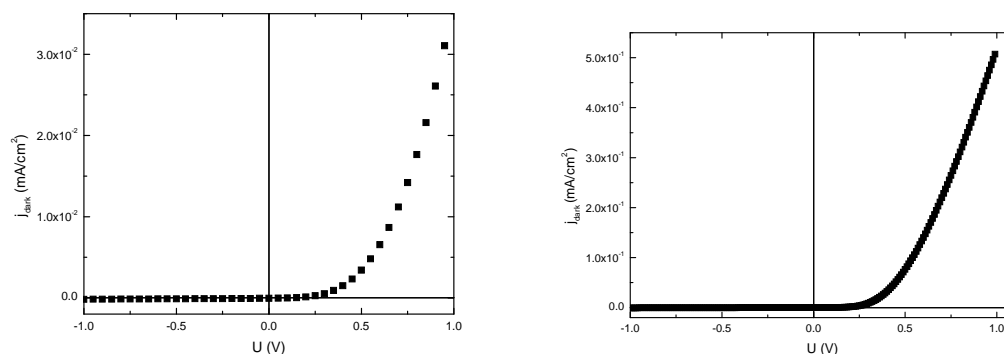


Fig. 5. Current-voltage characteristics for: ITO/CdS/CdTe (dry CdCl₂)/Cu/Au –left- respectively IZO/CdS/CdTe (wet CdCl₂)/Cu/Au –right-

After obtaining these current–voltage characteristics we started a study of the CdS / CdTe interface which is responsible for photovoltaic properties of the investigated structures. In order to do this we used the modified Shockley equation [27,29] given by:

$$I = I_o \{ \exp[\beta (V - IR_s)] - 1 \} + \frac{V - IR_s}{R_{sh}} \quad (1)$$

where: I_o is the reverse saturation current, R_s – the series resistance and R_{sh} – the shunt resistance. Here $\beta = q/nkT$, where q is the electronic charge, n – the diode quality factor, k – the Boltzmann constant, and T – the absolute temperature. Starting from this equation we can easily compute the differential resistance of the solar cell:

$$R_o = \frac{dV}{dI} = R_s + \frac{1}{\left\{ \beta I_o \exp[\beta(V - IR_s)] + \frac{1}{R_{sh}} \right\}} \quad (2)$$

At high voltages, in forward bias, equation (1) becomes $I = I_o \exp[\beta(V - IR_s)]$ and then equation (2) simplifies to:

$$R_o \cong R_s + \frac{1}{\beta I} \quad (3)$$

So, if we plot the dependencies of the differential resistance on the reciprocal of the current, at high voltages, the values for R_s and n parameters can be extracted (Figures 6 and 7).

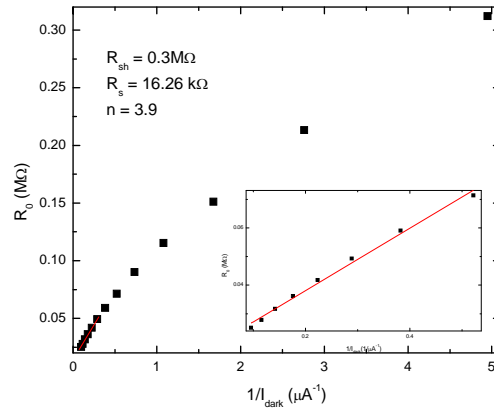


Fig. 6 – Dependence of the differential resistance of ITO/CdS/CdTe/Cu/Au cell on the reciprocal of the current at forward bias

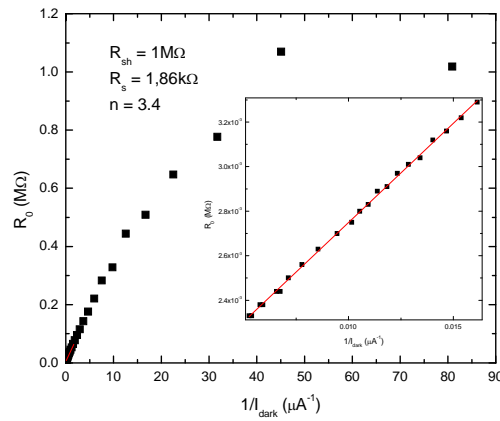


Fig. 7. Dependence of the differential resistance of IZO (AE2)/CdS/CdTe/Cu/Au cell on the reciprocal of the current at forward bias

At low voltages, where the current flowing through R_{sh} becomes important, equation (2) becomes $R_o \cong R_s + R_{sh}$. Since $R_s \ll R_{sh}$, it follows that R_o is essentially R_{sh} at low levels of injection.

On the other hand, the Shockley equation can be transformed as:

$$I - \frac{Y}{R_{sh}} = I_o [\exp(\beta Y)] \quad (4)$$

where: $I - \frac{Y}{R_{sh}}$ is the current flowing through the barrier and $Y = V - I R_s$ is the real voltage drop

across it. After we plot the dependencies of $\ln\left(I - \frac{Y}{R_{sh}}\right)$ on the real voltage Y , the linear part of this graph was extended and, after removing the effects of series and shunt resistances, we determined the I_o and n values.

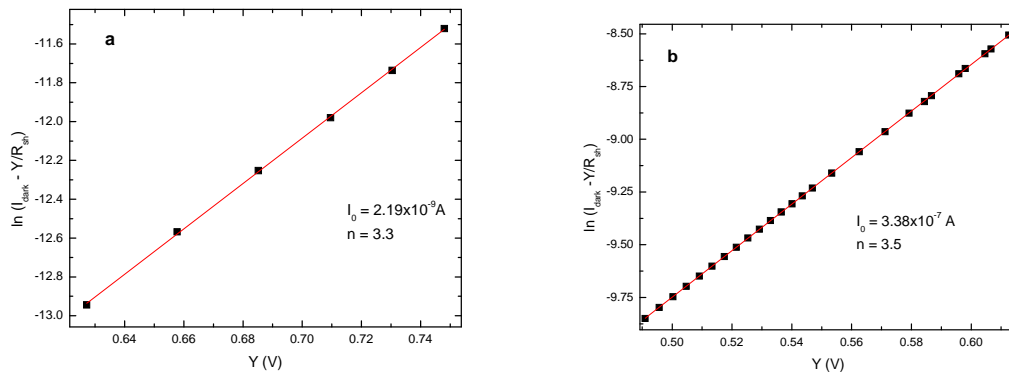


Fig. 8. The $\ln(I_{\text{dark}} - Y/R_{sh})$ vs $f(Y)$ characteristics for ITO/CdS/CdTe/Cu/Au – left – and IZO/CdS/CdTe/Cu/Au-right-

The values for series and shunt resistances, the reverse saturation current and the quality diode factor were calculated and are presented in Table 1 below.

Table 1– Parameters characterizing the CdS/CdTe heterojunction

Parameter	ITO/CdS/CdTe/Cu/Au	IZO/CdS/CdTe/Cu/Au
R_s (k Ω)	16.26	1.86
R_{sh} (M Ω)	0.3	1
I_0 (A)	2.19×10^{-9}	3.38×10^{-7}
n	3.3	3.5

4. Conclusions

Good quality polycrystalline CdS thin films have been obtained using thermal vacuum evaporation technique. The XRD studies confirmed the würtzite type structure of these films with crystallites sizes from 15 nm to 50 nm. The optical studies showed high transmittances of CdS thin films while the band-gap values are between 2.3 eV and 2.34 eV.

After these investigations entire photovoltaic structures ITO (or IZO) /CdS/CdTe/Cu/Au have been prepared and subjected to a complex series of thermal and chemical treatments. Cross-section SEM studies showed that these post-deposition treatments lead to some improved morphological properties (more smooth surfaces and more rounded grain facets).

From electric measurements and study of dark current – voltage characteristics the electric parameters (series and shunt resistances, the reverse saturation current and the quality diode factor) have been calculated for two kind of CdS/CdTe heterojunction solar cells.

The complex mixture of thermal and chemical treatments applied on obtained CdS / CdTe photovoltaic cells leads to the increasing of the inter-diffusion between the CdTe and CdS semiconductor layers and therefore to the improvement of the CdS–CdTe heterojunction, so we expect this to lead to a significant increase in solar cell efficiency.

Acknowledgements

This work was supported by the strategic grant POSDRU/89/1.5/S/58852, Project “Postdoctoral programme for training scientific researchers” co-financed by the European Social Found within the Sectorial Operational Program Human Resources Development 2007 – 2013.

References

- [1] S. Chun, K. S. Han, J. S. Lee, H. J. Lim, H. Lee, D. Kim, *Curr. Appl. Phys.* **10**, p. S196 (2010).
- [2] K. Ravichandran, P. Philominathan, *Appl. Surf. Sci.*, **255**, p. 5736 (2009).
- [3] A. Rotaru, A. M. Kropidłowska, C. Constantinescu, N. Scarisoreanu, M. Dumitru, M. Strankowski, P. Rotaru, V. Ion, C. Vasiliu, B. Becker, M. Dinescu, *Appl. Surf. Sci.*, **255**, p. 6786 (2009).
- [4] A. S. Khomane, *J. of Alloys and Comp.*, **496**, p. 508 (2010).
- [5] N. S. Das, P. K. Ghosh, M. K. Mitra, K. K. Chattopadhyay, *Physica E*, **42**, p. 2097 (2010).
- [6] H. Xie, C. Tian, W. Li, L. Feng, J. Zhang, L. Wu, Y. Cai, Z. Lei, Y. Yang, *Appl. Surf. Sci.*, **257**, p. 1623 (2010).
- [7] A. A. Yadav, M. A. Barote, E. U. Masumdar, *Solid State Sciences*, **12**, p. 1173 (2010).
- [8] J. Schaffner, E. Feldmeier, A. Swirschuk, H. J. Schimper, A. Klein, W. Jaegermann, *Thin Solid Films*, **519**, p. 7556 (2011).
- [9] M. C. Baykul, A. Balcioglu, *Microelectronic Engineering*, **51-52**, p. 703 (2000).
- [10] M. Ghenescu, L. Ion, I. Enculescu, C. Tazlaoanu, V. A. Antohe, M. Sima, M. Enculescu, E. Matei, R. Neumann, O. Ghenescu, V. Covlea, S. Antohe, *Physica E: Low-dimensional systems and Nanostructures*, **40**, p. 2485 (2008).
- [11] S. Antohe, L. Ion, V. A. Antohe, M. Ghenescu, H. Alexandru, *J. Optoelectron. Adv. Mater.*, **9**, p. 1382 (2007).
- [12] I. Enculescu, M. Sima, M. Enculescu, M. Enache, L. Ion, S. Antohe, R. Neumann, *Phys. Status Solidi (b)*, **244**, p. 1607 (2007).
- [13] L. Ion, S. Antohe, *J. Appl. Phys.* **97**, p. 3513 (2005).
- [14] S. Antohe, V. Ruxandra and H. Alexandru, *Journal of Crystal Growth*, **237-239**, p. 1559 (2002).
- [15] S. Antohe, L. Ion, V. A. Antohe, *Journal of Optoelectronics and Advanced Materials*, **5**, p. 801 (2003).
- [16] S. Antohe, L. Ion and V. Ruxandra, *J. Appl. Phys.*, **90**, p. 5928 (2001).
- [17] N. Romeo, A. Bosio, V. Canevari, A. Podesta, *Solar Energy*, **77**, p. 795 (2004).
- [18] A. Bylica, P. Sagan, I. Virt, G. Wysz, M. Bester, I. Stefaniuk, M. Kuzma, *Thin Solid Films*, **511-512**, p. 439 (2006).
- [19] K. W. Böer, *Energy Conversion and Management*, **52**, p. 426 (2011).
- [20] M. Tsuji, T. Aramoto, H. Ohyama, T. Hibino, K. Omura, *J. Cryst. Growth*, **214-215**, p. 1142 (2000).
- [21] N. Romeo, A. Bosio, A. Romeo, *Sol. En. Mat. and Solar Cells*, **94**, p. 2 (2010).
- [22] E. M. Feldmeier, A. Fuchs, J. Schaffner, H. J. Schimper, A. Klein, W. Jaegermann, *Thin Solid Films*, **519**, p. 7596 (2011).
- [23] V. Ruxandra, S. Antohe, *J. Appl. Phys.*, **84**, 2, p. 727 (1998).
- [24] L. Ion, V. Ghenescu, S. Iftimie, V. A. Antohe, A. Radu, M. Gugiu, G. Velisa, O. Porumb, S. Antohe, *Opt. Adv. Mat. Rap. Comm.*, **4**, 8, p. 1114 (2010).
- [25] L. Ion, I. Enculescu, S. Iftimie, V. Ghenescu, C. Tazlaoanu, C. Besleaga, T. L. Mitran, V. A. Antohe, M. M. Gugiu, S. Antohe, *Chalc. Lett.*, **7**, 8, p. 521 (2010).
- [26] O. Toma, R. Pascu, M. Dinescu, C. Besleaga, T. L. Mitran, N. Scarisoreanu, S. Antohe, *Chalc. Lett.*, **8**, 9, p. 541 (2011).
- [27] M. Radu, V. Ghenescu, I. Stan, L. Ion, C. Besleaga, A. Nicolaev, T. L. Mitran, C. Tazlaoanu, A. Radu, O. Porumb, M. Ghenescu, M. M. Gugiu, S. Antohe, *Chalc. Lett.*, **8**(8), 477 (2011).
- [28] A. R. Flores, J. L. Pena, V. C. Pena, O. Ares, R. C. Rodriguez, A. Basio, *Solar Energy*, **84**, 1020 (2010).
- [29] S. Antohe, V. Ruxandra, L. Tugulea, V. Gheorghe, D. Inascu, *J. Phys. III*, **6**, p. 1133 (1996).